

Screening length in plasma winds

Elena Caceres

Facultad de Ciencias,
Universidad de Colima,
Bernal Díaz del Castillo 340, Colima, Colima, Mexico
elenac@ucol.mx

Makoto Natsuume

Theory Division, Institute of Particle and Nuclear Studies,
KEK, High Energy Accelerator Research Organization,
Tsukuba, Ibaraki, 305-0801, Japan
makoto.natsuume@kek.jp

Takashi Okamura

Department of Physics,
Kwansei Gakuin University
Sanda, 669-1337, Japan
okamura@ksc.kwansei.ac.jp

Abstract: We study the screening length L_s of a heavy quark-antiquark pair in strongly coupled gauge theory plasma moving at velocity v . Using the AdS/CFT correspondence we investigate, analytically, the screening length in the ultra-relativistic limit. We develop a procedure that allows us to find the scaling exponent for a large class of backgrounds. We find that for conformal theories the screening length is (boosted energy density) $^{-1=d}$. As examples of conformal backgrounds we study R-charged black holes and Schwarzschild-anti-deSitter black holes in $(d+1)$ -dimensions. For non-conformal theories, we find that the exponent deviates from $-1=d$ and as examples we study the non-extremal Klebanov-Tseytlin and Dp-brane geometries.

Keywords: AdS/CFT correspondence, thermal field theory.

Contents

1. Introduction	1
2. General setup	3
2.1 Equations of motion	3
2.2 AdS/CFT dictionary	6
3. Leading behavior of the screening length	7
3.1 An example: $SA dS_5$	7
3.2 A formula for the scaling exponent	9
4. Conformal theories	11
4.1 R-charged black holes	11
4.2 The other dimensions	13
5. Non-conformal theories	13
5.1 Klebanov-Tseytlin geometry	13
5.2 Dp-branes	14
6. Discussion	16
7. Acknowledgments	17

1. Introduction

The analysis of the quark gluon plasma (QGP) produced in relativistic heavy ion collisions is, undoubtedly, a challenging task. One of the main difficulties is that in the temperature range of current and near-future experiments QCD is believed to be strongly coupled. Thus, one often focuses on the generic signatures of QGP. For example,

1. The elliptic flow
2. The jet quenching
3. $J=$ -suppression.

The first signature, the elliptic flow, is interpreted as a consequence of the QGP having a very low viscosity [1, 2]. In [3], Policastro, Son and Starinets pioneered the use of the AdS/CFT correspondence to study a strongly coupled plasma. It was found that the AdS/CFT prediction of the shear viscosity is in very good agreement with the value derived

from the elliptic flow [4]–[11]. This success indicates that AdS/CFT might be a good tool to gain some insight in the physics of QGP. It is thus natural to ask what are the AdS/CFT descriptions of the other QGP signatures and what can we learn from them. In fact, AdS/CFT descriptions of jet quenching and energy loss have been proposed recently [12]–[15]. (See Refs. [16]–[23] for extensions to other backgrounds and Ref. [20] for comparison of these different proposals. See also Ref. [24] for an early attempt.)

The next natural step is to investigate $J = \bar{c}c$ -suppression. Since $J = \bar{c}c$ is heavy, charm pair production occurs only at the early stages of the nuclear collision. However, if the production occurs in the plasma medium, charmonium formation is suppressed due to Debye screening. One technical difficulty is that the cc pair is not produced at rest relative to the plasma. Therefore, it is expected that the screening length will be velocity dependent. A dynamical calculation of the screening potential has been done only for the Abelian plasma [27].

Recently, there has been an interesting proposal by Liu, Rajagopal and Wiedemann to calculate the screening length via the AdS/CFT correspondence [25]. The authors considered a boosted black hole and computed the screening length in the quark-antiquark rest frame. In Ref. [26], the equivalent problem of a quark-antiquark pair moving in a thermal background was studied. The main lessons drawn from Ref. [25] are,

- (i) The screening length is proportional to (boosted energy density)^{-1/4}.
- (ii) Aside from the boost factor, $(1 - v^2)^{-1/4}$, the screening length has only a mild dependence on the wind velocity v .
- (iii) The length is minimum when $\theta = \pi/2$ and maximum $\theta = 0$, where θ is the angle of the quark-antiquark pair (dipole) relative to the plasma wind.

The main focus in Ref. [25] is the five-dimensional Schwarzschild-AdS black hole (SAdS₅), which is dual to the $N = 4$ super-Yang-Mills theory (SYM) at finite temperature. Even in that simple background, numerical computations were needed in order to see the full details of the screening length.

In this paper, we focus on the ultra-relativistic limit, where analytic computations are possible. This makes it easier to carry out the analysis in various, more involved, backgrounds. We study the scaling of the screening length with the energy density and the velocity. Our results are summarized as follows:

1. For conformal theories, we find the behavior

$$(\text{screening length}) / (\text{boosted energy density})^{-1/d}; \quad (1.1)$$

where d is the dimensions of the dual gauge theories. Examples are SAdS_{d+1} and R -charged black holes with three generic charges.

2. In particular, in the ultra-relativistic limit, the screening length at finite chemical potential is the same as the one at zero chemical potential for a given energy density.

3. For non-conformal theories,¹ the exponent deviates from $1=d$. Examples are the non-extremal Klebanov-Strömberg (KS) geometry and the Dp-brane solution. For the KS geometry, the deviation is proportional to the parameter of the nonconformality.

These results are in a sense natural; conformal theories have only few dimensionful parameters so the screening length should behave as Eq. (1.1) from dimensional grounds. On the other hand, non-conformal theories have other dimensionful parameters, so the screening length is not determined from dimensional analysis. However, even for conformal theories, the details are not determined from dimensional analysis alone. For example, in the ultra-relativistic limit the screening length in a R-charged black hole background, is independent of the chemical potential. Also, for non-conformal theories, the exponent turns out to be smaller than the one for the conformal examples.

In the next section, we will derive the relevant equations of motion for general backgrounds. We then proceed to analyze conformal theories in Sec. 4, where we also develop a general procedure to treat a large class of backgrounds. As examples, we calculate the screening length for R-charged black holes and $SAdS_{d+1}$. In Sec. 5, we analyze two non-conformal theories: the non-extremal KS solution and Dp-branes backgrounds. We conclude in Sec. 6 with discussion, implications and future directions.

2. General setup

In the AdS/CFT framework, a heavy quark may be realized by a fundamental string which stretches from the asymptotic infinity (or from a "flavor brane") to the black hole horizon. This string transforms as a fundamental representation; in this sense, the string represents a "quark." The fundamental string has an extension and the tension, so the string has a large mass, which means that the string represents a heavy quark.

For a qq pair, two individual strings extending to the boundary is not the lowest energy configuration. Instead, it is energetically favorable to have a single string that connects the pair. The energy difference is interpreted as a qq potential and has been widely studied in the past from the AdS/CFT perspective. At finite temperature [28, 29], it is no longer true that a string connecting the qq pair is always the lowest energy configuration; for large enough separation of the pair, isolated strings are favorable energetically. This phenomenon is the dual description of Debye screening in AdS/CFT. In Ref. [25], the authors computed qq potential in the qq rest frame, i.e., they considered the plasma flowing at a velocity v . Such a "plasma wind" is obtained by boosting a black hole background.

2.1 Equations of motion

In order to consider the screening length in the dipole rest frame we boost the background metric. We assume an unboosted metric of the form

$$ds^2 = g_{xx} f(1-h) dt^2 + dx_{\perp}^2 g + g_{rr} dr^2 + \dots \quad (2.1)$$

¹In this paper, we use the word "non-conformal" for a theory with nontrivial dilaton.

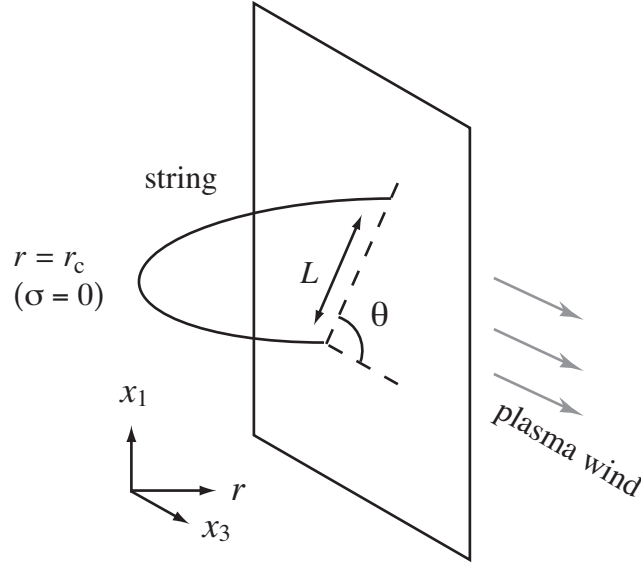


Figure 1: The fundamental string connecting the quark-antiquark pair. (The shape of the string should not be taken seriously.)

Consider the plasma wind in the x_3 -direction, so the boosted metric is

$$ds^2 = (1 - h^2) dt^2 + dx_3^2 - 2h \cosh \alpha dt dx_3 + (1 + h^2 \sinh^2 \alpha) dx_3^2; \quad (2.2)$$

where v is the wind velocity, $\cosh \alpha = \frac{1}{\sqrt{1 - v^2}}$, $\sinh \alpha = \frac{v}{\sqrt{1 - v^2}}$, and $h = \frac{p}{1 - v^2}$.

The dynamics of the fundamental string is governed by the Nambu-Goto action. The quark-antiquark pair is chosen to lie in the $(x_1; x_3)$ -plane at an angle θ relative to the wind (See Fig. 1). Thus, we choose the gauge $\tau = t$; $\sigma = x_1$ and consider the configuration

$$x_3 = x_3(\sigma); \quad r = r(\sigma); \quad \text{constant otherwise}; \quad (2.3)$$

Then, the Nambu-Goto action (in the string metric²) becomes

$$S = \frac{1}{2\pi\alpha'} \int d^2\sigma \sqrt{-\det G_{ab}} \quad (2.4)$$

$$= \frac{1}{2\pi\alpha'} \int d^2\sigma \sqrt{-G_{00}(G_{11} + G_{33}x_3'^2 + G_{rr}r'^2) + G_{03}^2 x_3'^2}; \quad (2.5)$$

Here, we used the boosted metric components such as G_{03} and $G_{00} = d = d^2$. The conserved quantities are

$$q = \frac{\partial L}{\partial r^0} r'^0 + \frac{\partial L}{\partial x_3^0} x_3'^0 = L; \quad (2.6)$$

$$p = \frac{\partial L}{\partial x_3^0}; \quad (2.7)$$

²In this paper, we mostly use the string metric. If one would like to work in the $d = 10$ Einstein metric, simply make the following replacements in all formulae in this subsection: $g_{xx} \rightarrow e^{-2\phi} g_{xx}$; $g_{rr} \rightarrow e^{-2\phi} g_{rr}$.

which become

$$q^2 r^2 = \frac{g_{xx}}{g_{rr}} \frac{1 - h \cosh^2}{1 - h} g_{xx}^2 (1 - h) p^2 q^2 = : F(y); \quad (2.8)$$

$$q x_3^0 = p \frac{1 - h \cosh^2}{1 - h}; \quad (2.9)$$

or equivalently,

$$x_1 = \int^Z \frac{dr}{F}; \quad (2.10)$$

$$\begin{aligned} x_3 &= \int^Z \frac{dx_3}{dr} dr = p \int^Z \frac{dr}{F} \frac{1 - h \cosh^2}{1 - h} \\ &= p \frac{x_1}{q} \sinh^2 \int^Z \frac{dr}{F} \frac{h}{1 - h}; \end{aligned} \quad (2.11)$$

The string stretches from asymptotic infinity and reaches a turning point $r = r_c$ defined by $F(r_c) = 0$. Then, the string goes back to asymptotic infinity. From the symmetry, the turning point occurs at $\theta = 0$. Then the boundary conditions are summarized as,

$$\begin{aligned} r(\theta = 0) &= r_c; & F(r_c) &= 0; \\ r(\theta = L \sin \frac{\pi}{2}) &= 1; & x_3(\theta = L \sin \frac{\pi}{2}) &= \frac{L}{2} \cos \frac{\pi}{2}; \end{aligned} \quad (2.12)$$

where L is the dipole length. The boundary conditions determine the integration constants p and q in terms of L and r_c :

$$\frac{L}{2} \sin \frac{\pi}{2} = q I_s(p; q; r_c); \quad (2.13)$$

$$\frac{L}{2} \cos \frac{\pi}{2} = p I_c(p; q; r_c) \sinh^2 \frac{\pi}{2}; \quad (2.14)$$

where

$$I_s(p; q; r_c) = \int_{r_c}^Z \frac{dr}{F}; \quad (2.15)$$

$$I_c(p; q; r_c) = \int_{r_c}^Z \frac{dr}{F} \frac{h}{1 - h}; \quad (2.16)$$

The energy is given by

$$\begin{aligned} E &= \frac{S}{T} \\ &= \frac{1}{L_s} \int_{r_c}^Z dr \frac{q}{g_{xx} g_{rr} (1 - h \cosh^2)} \sqrt{\frac{g_{xx}}{g_{rr} F} \left(q^2 + p^2 \frac{1 - h \cosh^2}{1 - h} \right) + 1}; \end{aligned} \quad (2.17)$$

As usual, this energy can be made finite by subtracting the self-energy of a disconnected quark and antiquark pair which is

$$E_0 = \frac{1}{L_s} \int_{r_0}^Z \frac{q}{g_{xx} g_{rr} (1 - h \cosh^2)}; \quad (2.18)$$

where r_0 is the location of the horizon.

Two special cases are worth discussing separately.

(i) $\alpha = -2$: This is the case when the plasma wind is perpendicular to the dipole. In this case, Eq. (2.14) implies $p = 0$. The integration constant q can be determined from

$$L = 2q \int_{r_c}^{Z_1} \frac{p \sqrt{g_{rr}} dr}{g_{xx} f(1 - h \cos^2 \theta) g_{xx}^2} : \quad (2.19)$$

(ii) $\alpha = 0$: This is the case when the plasma wind is parallel to the dipole. In this case, Eq. (2.13) implies $q = 0$. Then,

$$L = 2p \int_{r_c}^{Z_1} dr p \frac{1}{F} \frac{1}{h} \frac{h \cos^2 \theta}{1 - h} : \quad (2.20)$$

2.2 AdS/CFT dictionary

Some well-known AdS/CFT dictionary is summarized here. This dictionary is valid for AdS₅, R-charged black holes, and the Dp-brane. Roughly speaking, on the left-hand side we have gravity quantities which are written in terms of gauge theory quantities on the right-hand side.

$$16 G_{10} = (2)^7 g_s^2 l_s^8 ; \quad (2.21)$$

$$R^{7-p} = \frac{(2)^{7-p}}{(7-p) 8^p} g_s N_c^{1/8-p} \quad (R \text{ in terms of } N_c); \quad (2.22)$$

$$2(2)^p g_s^2 l_s^3 = g_{YM}^2 \quad (g_s \text{ in terms of } g_{YM}); \quad (2.23)$$

where

G_{10} : 10-dimensional Newton constant

g_s : string coupling

R : AdS radius

N_c : number of colors

g_{YM} : YM coupling

S^n volume of unit radius; $V_n = 2 \frac{\pi^{n+1}}{2} = (\frac{n+1}{2})$:

When $p = 3$,

$$16 G_{10} = (2)^7 \frac{R^8}{(4 N_c)^2} ; \quad (2.24)$$

$$(R=l_s)^4 = ; \quad (2.25)$$

where g_5 is the 5d Newton constant. Below we often consider effective 5-dimensional theories with the 5-dimensional Newton constant given by

$$G_5 = \frac{G_{10}}{R^5} = \frac{R^3}{2N_c^2} : \quad (2.26)$$

3. Leading behavior of the screening length

3.1 An example: SA dS₅

As an example, let us start with the SA dS₅ case. This has been studied numerically in Ref. [25]. Here we study it analytically in the ultra-relativistic limit. The SA dS₅ black hole is given by

$$ds^2 = \frac{r^2}{R^2} dt^2 + \frac{r_0^4}{r} \left(\frac{dr^2}{\frac{r^2}{R^2} f(r)} + \frac{r^2}{R^2} (dx_1^2 + dx_2^2 + dx_3^2) \right) \quad (3.1)$$

The temperature T and the (unboosted) energy density ρ_0 of the black hole are given by

$$T = \frac{r_0}{R^2}; \quad (3.2)$$

$$\rho_0 = \frac{3}{16 G_5} \frac{r_0^4}{R^5} = \frac{3}{8} N_c^2 T^4; \quad (3.3)$$

For $\nu = 2$, Eq. (2.19) becomes

$$L_{\text{SA dS}}(\nu = 2) = 2\hat{q} \frac{R^2}{r_0} \int_{y_c}^{\infty} dy \frac{1}{y^2 \sqrt{y^4 - 1} \sqrt{y^4 - y_c^4}}; \quad (3.4)$$

where we used the dimensionless variables

$$y = \frac{r}{r_0}; \quad \hat{q} = \frac{R^2}{r_0} q; \quad \hat{p} = \frac{R^2}{r_0} p; \quad (3.5)$$

and y_c is the turning point given by $y_c^4 = \cosh^2 \hat{q} + \hat{q}^2$.

The above integral Eq. (3.4) can be evaluated numerically but is slightly involved since one is interested in $L_{\text{SA dS}}$ as a function of q . We choose not to follow the numerical route; instead, we investigate analytically the ultra-relativistic limit of Eq. (3.4). For large \hat{q} , $y_c \gg 1$, so the integral reduces to

$$L_{\text{SA dS}}(\nu = 2) \approx \frac{1}{2} \frac{R^2}{r_0} \int_{y_c}^{\infty} dy \frac{1}{y^2 \sqrt{y^4 - y_c^4}} \quad (3.6)$$

$$= \frac{1}{2} \frac{R^2}{r_0} \frac{\hat{q}}{(\cosh^2 \hat{q} + \hat{q}^2)^{3/4}}; \quad (3.7)$$

We are interested in the behavior of $L_{\text{SA dS}}$ as a function of \hat{q} . The length $L_{\text{SA dS}}$ goes to zero both for small \hat{q} and for large \hat{q} . Thus, there is a maximum value L_s at some \hat{q}_m . This means that there is no extremal world-sheet which binds the quark-antiquark pair for $L > L_s$, so this L_s is defined as a screening length in Ref. [25]. The maximum of $L_{\text{SA dS}}$ is given by

$$L_s^{\text{SA dS}}(\nu = 2) = \frac{1}{2} \frac{R^2}{r_0} \frac{\hat{q}_m}{(\cosh^2 \hat{q}_m + \hat{q}_m^2)^{3/4}} \quad \text{at } \hat{q}_m = \sqrt{2} \cosh \hat{q}_m \quad (3.8)$$

$$= \frac{0.743}{\cosh \hat{q}_m} \frac{R^2}{r_0}; \quad (3.9)$$

Rewriting in terms of gauge theory variables, the screening length L_s is given by

$$L_s^{\text{SA dS}} (\epsilon = 2) = \frac{0.743}{\mathfrak{p}} \frac{1}{T} : \quad (3.10)$$

This parametrization in terms of temperature was adopted in Ref. [25]. One can equally express the result in terms of energy density:

$$L_s^{\text{SA dS}} (\epsilon = 2) = \frac{2^{3=4}}{\mathfrak{p}} \frac{(3=4)}{(1=4)} \frac{\mathfrak{p} \overline{N_c}}{(\epsilon \cosh^2)^{1=4}} \quad (3.11)$$

$$0.328 \frac{\mathfrak{p} \overline{N_c}}{(\epsilon \cosh^2)^{1=4}} : \quad (3.12)$$

The choice of these parametrizations does not matter for SA dS₅ since there is no other dimensionful quantities. But it does matter when one has other dimensionful quantities such as the chemical potential. Our results in the next section strongly indicate that one should really choose the energy density to parametrize the screening length. However, one drawback of doing so is that the results will depend also on N_c (and for D p-branes), so they have no finite large- N_c limit. If one chooses T , they do not appear explicitly and appear only through T .

A few comments are in order. The temperature dependence in Eq. (3.10) is very natural and is the same as the standard Debye length. In terms of the energy density, $\mathfrak{p} \overline{N_c}$ appears in the expression because $\epsilon / N_c^2 T^4$ (both in the weak coupling and in the strong coupling as first noted by Gubser, Klebanov, and Peet [30].) On the other hand, the expressions have no dependence on the coupling and are in contrast to the naive weak coupling result $L_s / g_{YM} \mathfrak{p} \overline{N_c} T$. This is due to the large- N_c limit and there should be coupling dependences such as $\epsilon^{3=2}$ from the next order.

For $\epsilon = 0$, Eq. (2.20) becomes

$$L_{\text{SA dS}} (\epsilon = 0) = 2\mathfrak{p} \frac{R^2}{r_0} \int_{y_c}^{\infty} \frac{dy}{y^4} \sqrt{1 - \frac{y^4}{y_c^4}} ; \quad (3.13)$$

where $y_c^4 = 1 + \mathfrak{p}^2$. In order for the function inside the square-root not to become negative, $y_c > \frac{\mathfrak{p}}{\cosh}$. This suggests \mathfrak{p} is large in this case. In terms of the rescaled variables $\hat{\mathfrak{p}} = \frac{\mathfrak{p}}{\cosh}$ and $y = \frac{\mathfrak{p}}{\cosh} \tilde{y}$, the above integral in the large- \mathfrak{p} limit becomes

$$L_{\text{SA dS}} (\epsilon = 0) = \frac{2\mathfrak{p}}{\cosh} \frac{R^2}{r_0} \int_{\hat{\mathfrak{p}}}^{\infty} \frac{d\tilde{y}}{\tilde{y}^4} \sqrt{1 - \frac{1}{\hat{\mathfrak{p}}^2}} : \quad (3.14)$$

The above integral can be evaluated numerically. The maximum of $L_{\text{SA dS}}$ is given by

$$L_s^{\text{SA dS}} (\epsilon = 0) = \frac{0.838}{\cosh} \frac{R^2}{r_0} \quad \text{at } \hat{\mathfrak{p}}_m = 1.38 \cosh \quad (3.15)$$

$$0.370 \frac{\mathfrak{p} \overline{N_c}}{(\epsilon \cosh^2)^{1=4}} : \quad (3.16)$$

Hence, the screening length increases for the wind parallel to the dipole compared with the screening length for the wind perpendicular to the dipole as was observed numerically by Ref. [25].

Note also that doing a numerical fit to find the scaling at large velocities can be misleading. In fact, in Ref. [26], the authors found that the numerical fit valid for all the range $0 < v < 1$ scales like $(1 - v^2)^{1=3}$. This could lead us to believe that $(1 - v^2)^{1=3}$ is also the correct scaling for large v . We have seen that this is not the case. Analytically examining the behavior of L_s in different limits is a powerful tool; We will apply it in the next sections to find the scaling of L_s as $v \rightarrow 1$.

3.2 A formula for the scaling exponent

An analysis similar to the previous subsection is straightforward with the other backgrounds. Instead of studying each background one by one, we will develop a general formalism to find the scaling exponent.

We start with Eqs. (2.13)–(2.16) and F defined by Eq. (2.8),

$$F(r) = \frac{g_{xx}(r)}{g_{rr}(r)} \frac{1 - h(r) \cosh^2}{1 - h(r)} \frac{g_{xx}^2(r) - 1 - h(r) - p^2 - q^2}{p^2 - q^2} ;$$

The turning point r_c is defined by $F(r_c) = 0$ and satisfies

$$\cosh^2 = \frac{1}{h(r_c)} \frac{1 - q^2}{g_{xx}^2(r_c) - 1 - h(r_c) - p^2} ; \quad (3.17)$$

We assume that the metric falls off

$$g_{xx}(r) = \frac{r}{R}^\alpha ; \quad g_{rr} = C^2 \frac{r}{R}^\beta ; \quad h(r) = \frac{m}{r^h} = \frac{m}{R^h} \frac{r}{R}^{-h} ; \quad (3.18)$$

near the infinity $r = 1$. The parameter m is the mass parameter. A priori there is no reason to regard it as the energy density, but in our examples below, it in fact represents the energy density. Furthermore, we assume that the metric behaves as³

$$g_{xx}^2 \sim h \quad (\text{at most } O(1)) ; \quad g_x \quad (\text{divergent}) ; \quad (3.19)$$

If $\alpha; h > 0$, the turning point satisfies $h(r_c) \rightarrow 1$ for large- from Eq. (3.17),⁴ more precisely, $0 - h(r_c) = 0 - 1 = \cosh^2$, so that the turning point is near the infinity. We are interested in the leading order term of \cosh , so we need only the leading term of the metric.

Using the parameter,

$$E = \frac{m \cosh^2}{R^h} ; \quad (3.20)$$

³If one chooses the radial coordinate r used for the SAdS₅, this condition is equivalent to the condition $h - 2\alpha > 0$.

⁴The function, $g(r) = g_{xx}^2(r) (1 - h(r)) - p^2$, does not vanish. Because the string has its end points at the infinity and $g(1) = +1$, the function $g(r)$ approaches to zero with positive value. If $g(r)$ became positive in infinitesimal value, the RHS of Eq. (3.17) would be negative.

the function F behaves as

$$F \approx \frac{1}{C^2} \frac{r}{R} \left(\frac{x+r}{R} \right)^{-1} \approx \frac{1}{E} \frac{r}{R} \left(\frac{r}{R} \right)^{-2} \frac{x}{R} \approx \frac{p^2}{q^2} \quad ; \quad (3.21)$$

Using the rescaled variables⁵

$$t \equiv \frac{(r=R)}{E} \quad ; \quad p^2 \equiv \frac{p^2}{E^2 x=h} \quad ; \quad q^2 \equiv \frac{q^2}{E^2 x=h} \quad ; \quad (3.22)$$

we can rewrite Eqs. (2.13) and (2.14) as

$$\frac{L}{R} \sin \left(\frac{2C}{h} E \right) \approx \mathcal{I}_s(p; q) \quad ; \quad (3.23)$$

$$\frac{L}{R} \cos \left(\frac{2C}{h} E \right) \approx \mathcal{I}_s(p; q) \mathcal{I}_c(p; q) \quad ; \quad (3.24)$$

where

$$\mathcal{I}_s(p; q) \equiv \int_{t_c}^Z \frac{dt}{t} \frac{t^{1=2}}{(t-1) \left(\frac{t}{p} \right) \left(\frac{t}{q} \right)} \quad ; \quad (3.25)$$

$$\mathcal{I}_c(p; q) \equiv \int_{t_c}^Z \frac{dt}{t} \frac{t^{1=2}}{(t-1) \left(\frac{t}{p} \right) \left(\frac{t}{q} \right)} \quad ; \quad (3.26)$$

and

$$\frac{x+r}{2h} \approx \frac{x}{h} \frac{1}{2} \quad ; \quad (3.27)$$

The turning point $t_c = \max(p^2, 1)$ is then determined by

$$0 = (t_c - 1) t_c^2 \frac{p^2}{q^2} \quad ; \quad (3.28)$$

Equations (3.23) and (3.24) imply that the maximum of L, L_s , behaves as

$$L_s / RE \approx R \frac{m}{R h} \cosh^2 \quad (3.29)$$

irrespective of β . Since the parameter m is related to the energy density in our examples, the screening length L_s is written in terms of the boosted "energy density" of plasma wind at large β .⁶ Below we compute the exponent β in various theories.

Finally, let us briefly discuss the radial-coordinate dependence of our formulae. We used the radial coordinate r for $SA dS_5$ and one may use a similar coordinate which approaches r asymptotically when one considers more general backgrounds. But it is sometimes more convenient to use a coordinate other than r (See, e.g., the KT geometry in

⁵For $SA dS_5$, the coordinate t is related to the coordinate \bar{y} (used in Sec. 3.1) by $\bar{y}^4 = t$. The definition of conserved quantity p coincides with the one for $SA dS_5$.

⁶One may wonder if L_s is always written in terms of the combination \cosh^2 . This question however is not a well-defined one when the other dimensional quantities exist, so one should not take the combination very seriously. The exponent β must be understood as the power of the (squared) Lorentz factor, \cosh^2 .

Sec. 5.1). Thus, let us check if the choice of a coordinate affects our discussion. When we derive Eq. (3.29), we used only the power-law behavior of the metric (3.18). Also, the equations of motion, e.g., Eqs. (2.10) and (2.11) themselves are invariant under the reparametrization of the radial coordinate r . This is because the g_{rr} -component appears only in the form of $\int^D \frac{1}{g_{rr}} dr$. The power-law behavior together with the reparametrization invariance suggest that one is free to choose any radial coordinate as long as the metric has a power-law behavior. Indeed, consider a new coordinate r such as

$$\frac{r}{R} = \frac{r}{R} (1 + O[(R=r)^a]); \quad a > 0 \quad (3.30)$$

and define new power indices α_i ; β_r and β_h . The new indices still satisfy the condition (3.19) even if $\alpha < 0$. One can easily check that the physical indices are all unchanged:

$$\alpha_i = \alpha_i; \quad \beta_r = \beta_r; \quad \frac{C}{h} = \frac{C}{h}; \quad (3.31)$$

Therefore, our formulae are not affected by the choice of radial coordinate; One can choose a radial coordinate at will as long as the metric has a power-law behavior.

4. Conformal theories

For conformal theories, our results are consistent with the behavior

$$(\text{screening length}) / (\text{boosted energy density})^{1=d}; \quad (4.1)$$

where d is the dimensions of the dual gauge theories.

4.1 R-charged black holes

As a first example, consider five-dimensional black holes charged under the R-symmetry group $U(1)_R^3$. These backgrounds are dual to the $N = 4$ SYM with chemical potentials. The three-charge STU-solution (with noncompact horizon) is specified by the following background metric:⁷

$$ds^2 = H^{-2=3} f dt^2 + H^{1=3} f^{-1} dr^2 + H^{1=3} \frac{r}{R}^2 (dx_1^2 + dx_2^2 + dx_3^2); \quad (4.2)$$

where

$$f = \frac{r^2}{R^2} + \frac{r^2}{R^2} H; \quad H_i = 1 + \frac{C_i}{r^2}; \quad H = H_1 H_2 H_3; \quad (4.3)$$

The outer horizon r_+ is given by the larger root of $f(r) = 0$. The three R-charges c_i are related to the angular momenta l_i in 10-dimensions, $c_i = l_i^2$.

⁷In this paper, we consider the string which satisfies the ansatz Eq. (2.3), namely the string is fixed in the compact dimensions when embedded into 10-dimensions. This means that the string we consider is not charged under the R-charges.

When three charges are equal, $c_i = c$, the STU-solution reduces to the Reissner-Nordstrom-AdS₅ (RN-AdS₅) black hole. The standard form of the RN-AdS₅ black hole is written as

$$ds^2 = -f(r)dt^2 + f^{-1}(r)dr^2 + \frac{r}{R}{}^2(dx_1^2 + dx_2^2 + dx_3^2); \quad (4.4)$$

$$f(r) = \frac{r}{R}{}^2 - \frac{m_{RN}}{r^2} + \frac{Q_{RN}^2}{r^4}; \quad (4.5)$$

This form is related to the STU-solution by a coordinate transformation $r^2 + c = r'^2$ with $m_{RN} = m$ and $c = Q_{RN}^2$.

The temperature T and the energy density ρ_0 of the black hole are given by

$$T_H = \frac{2 + \frac{1}{2} + \frac{2}{2} + \frac{3}{2} - \frac{1}{2} - \frac{2}{2} - \frac{3}{2}}{2^{\frac{1}{2}} (1 + \frac{1}{2}) (1 + \frac{2}{2}) (1 + \frac{3}{2})} T_0; \quad (4.6)$$

$$\rho_0 = \frac{3}{16 G_5 R^5} \frac{r_+^4 Y^3}{\prod_{i=1}^3 (1 + \frac{r_+^2}{c_i})} = \frac{3}{8} \frac{2N^2 T_0^4 Y^3}{\prod_{i=1}^3 (1 + \frac{r_+^2}{c_i})}; \quad (4.7)$$

where \tilde{c}_i is not the physical charge but the rescaled charge $\tilde{c}_i = c_i/r_+^2$.

The fall-off behavior of the STU-solution is

$$g_{xx} \sim \frac{r}{R}{}^2; \quad g_{rr} \sim \frac{r}{R}{}^2; \quad h \sim \frac{Y^3}{\prod_{i=1}^3 (1 + \frac{r_+^2}{c_i})} \frac{r_+^4}{r}{}^4; \quad (4.8)$$

thus $\alpha_x = \alpha_r = 2$, $\alpha_h = 4$, and $m = r_+^4 \prod_{i=1}^3 (1 + \frac{r_+^2}{c_i}) / \rho_0$ from Eq. (4.7). The fall-off behavior satisfies the condition (3.19). Note that m becomes complicated if one wants to write it in terms of charges and temperature. From Eq. (3.27), we get

$$R = \frac{\alpha_x + \alpha_r}{2 \alpha_h} = \frac{1}{4}; \quad (4.9)$$

and Eq. (3.29) is written as

$$L_s^R / \frac{p}{N_c} : \quad (4.10)$$

Moreover, note that the screening length is exactly the same as the SAdS₅ case at a given energy density because the expressions (3.23)–(3.27) do not change. In particular, the results for SAdS_d, (3.11) and (3.15), also hold for any R-charged black hole without modifications. This is because only the leading behavior of the metric matters by taking the ultra-relativistic limit as we saw in Sec. 3.2. The leading behavior depends only on the energy density, not on the charge. [For example, see Eq. (4.5).] This suggests that it is more appropriate to define the screening length L_s as

$$L_s / \frac{f(v)}{1=4} (1 - v^2)^{1=4} \quad (4.11)$$

rather than using the temperature for generic case.

4.2 The other dimensions

Let us briefly look at gauge/gravity duals in the other dimensions to see the dimensional dependence on the screening length. As an example, consider the SA dS_{d+1} black hole given by

$$ds^2 = \frac{r^2}{R^2} dt^2 + \frac{r_0^d}{r} dr^2 + \frac{r^2}{R^2} (dx_1^2 + \dots + dx_{d-1}^2) \quad (4.12)$$

We assume d ≥ 4. This black hole is dual to a d-dimensional conformal field theory at finite temperature. But we do not specify the precise duals since the main purpose here is just to look at dimensional dependence on the screening length.⁸

The temperature T and the energy density ρ of the black hole are given by

$$T = \frac{d}{4 R^2} r_0 \quad ; \quad (4.13)$$

$$\rho = \frac{d}{16 G_{d+1}} \frac{r_0^d}{R^{d+1}} \quad ; \quad (4.14)$$

where G_{d+1} is the (d + 1)-dimensional Newton constant.

The fall-off behavior of the SA dS_{d+1} is

$$g_{xx} = \frac{r^2}{R^2} \quad ; \quad g_{rr} = \frac{r}{R} \quad ; \quad h = \frac{r_0^d}{r} \quad ; \quad (4.15)$$

thus $\alpha = \beta = 2$, $\gamma = d$, and $m = r_0^d / \rho$. The fall-off behavior satisfies the condition (3.19). Thus, $\alpha_{SA dS} = 1=d$ and

$$L_S / \frac{1}{T (\cosh^2)^{1=d}} / R = \frac{1}{G_{d+1} R} = \frac{1}{(\rho \cosh^2)^{1=d}} \quad ; \quad (4.16)$$

5. Non-conformal theories

We now move on to non-conformal theories; We will see in the following examples that the exponent deviates from 1=d.

5.1 Klebanov-Teitelboim geometry

As an example of non-conformal theories, consider the KT geometry, which is dual to N = 1 cascading SU(K) × SU(K + P) gauge theory. The finite temperature solution, for temperatures high above the deconfining transition, was constructed in [31, 32, 33]. The 10-dimensional metric (in the Einstein metric) is given by

$$ds_E^2 = \frac{P}{8a=K} e^{2P^2} (1 - z)^2 dt^2 + dx_i^2 + \frac{P}{32} e^{-2P^2} \left(\frac{dz^2}{z^2 (1 - z)} + \dots \right) \quad ; \quad (5.1)$$

⁸ Some examples are SA dS₄ × S⁷ and SA dS₇ × S⁴ in M-theory, which correspond to the M2-brane and M5-brane, respectively. Of course, it does not really make sense to use the fundamental string in the context of M-theory.

where $\frac{1}{2} \log z$ stands for the compact $(d-1)$ -dimensional part and the radial coordinate z runs from the horizon $z = 1$ to the asymptotic infinity $z \rightarrow \infty$. The solution is valid to the first order in $P^2 = K^{-1}$. The solution is known for all range of z ($0 < z < \infty$). In Ref. [34], it was argued that to study in detail the solution in the interval $z < z_c$, where z_c is a very small but nonzero number, a numerical analysis is necessary. We will only be concerned with the leading terms in the metric which are summarized in Eqs. (5.22), (5.30), and (5.31) of Ref. [31].

$$\frac{\log z}{8K} + O(z^{-1}); \quad (5.2)$$

$$O(z^{-2}); \quad (5.3)$$

$$O(z^{-3} \ln z); \quad (5.4)$$

As discussed at the end of Sec. 3.2, one can use the coordinate z to find the exponent. Then,

$$x = \frac{P^2}{4K} \frac{1}{2}; \quad z = \frac{P^2}{4K} + 2; \quad h = 1; \quad (5.5)$$

Thus,

$$K_T = \frac{1}{4} \frac{P^2}{K} < \frac{1}{4}; \quad (5.6)$$

Note that even though K_T is dual to a four dimensional gauge theory, the exponent we find in this case deviates from $d=4$. This deviation is measured by $\frac{P^2}{K}$ which is a non-conformality parameter. Thus, the fact that the scaling exponent is less than $d=4$ for a K_T background is intimately related with the non-conformal nature of the theory.

5.2 D p-branes

In the previous subsection, we saw that the exponent deviates from $d=4$ for a non-conformal theory. In order to see how large the deviation can be, it is desirable to study theories with strong deviation from the conformality. When the deviation is small, many examples are known. Unfortunately, few theories are known when the deviation is large; the D p-brane is one such example. The D p-brane background is dual to the $(p+1)$ -dimensional SYM with 16 supercharges. (For a recent discussion of this duality, see Ref. [35] and references therein.) In the string metric, the near-horizon limit of the D p-brane geometry (for $p < 7$) is given by

$$ds^2 = \frac{r}{R} \frac{r_0^{7-p}}{r^{7-p}} dt^2 + \frac{r}{R} \frac{r_0^{7-p}}{r^{7-p}} (dx_1^2 + \dots + dx_p^2) + \frac{dr^2}{\left(\frac{r}{R}\right)^{\frac{7-p}{2}} f_1 \frac{r_0^{7-p}}{r^{7-p}} g} + R^2 \frac{r}{R} \frac{r_0^{\frac{p-3}{2}}}{r^{\frac{p-3}{2}}} d^{\frac{8-p}{2}} \Omega_p; \quad (5.7)$$

The $p = 3$ case is the SA dS₅ solution. The temperature T and the energy density ρ_0 of the black hole are given by

$$T = \frac{(7-p)r_0^{\frac{5-p}{2}}}{4R^{\frac{7-p}{2}}}; \quad (5.8)$$

$$\rho_0 = \frac{9-p}{32G_{10}} r_0^{7-p} / \frac{p-3}{5-p} N_c^2 T^{\frac{2(7-p)}{5-p}}; \quad (5.9)$$

The fall-off behavior of the Dp-branes is

$$g_{xx} = \frac{r}{R}^{\frac{7-p}{2}}; \quad g_{rr} = \frac{r}{R}^{\frac{7-p}{2}}; \quad h = \frac{r_0}{r}^{7-p}; \quad (5.10)$$

thus $\alpha_x = \alpha_r = (7-p)/2$, $\alpha_h = 7-p$, and $m = r_0^{7-p} / \rho_0$. The fall-off behavior satisfies the condition (3.19). Thus,

$$L_s^{Dp} = \frac{5-p}{2(7-p)} \quad (5.11)$$

and

$$L_s^{Dp} / \frac{1}{T (\cosh^2)^{\frac{5-p}{2(7-p)}}} / \frac{\frac{p-3}{5-p} N_c^2}{\rho_0 \cosh^2} \frac{r_0^{\frac{5-p}{2(7-p)}}}{r^{\frac{5-p}{2(7-p)}}}; \quad (5.12)$$

For $p = 2$, it is easy to carry out the integral (3.23) and one gets

$$L_s^{Dp} (p=2) = p \frac{2^{p-1}}{(5-p)(7-p)} \frac{5-p}{2(6-p)} \frac{r_0^{\frac{6-p}{7-p}}}{\left(\frac{3}{2}\right)^{\frac{1}{7-p}}} \frac{R}{f\left(\frac{r_0}{R}\right)^{7-p} \cosh^2} \frac{1}{g^{\frac{5-p}{2(7-p)}}}$$

$$\text{at } q_m = \frac{r}{\frac{7-p}{5-p} \frac{r_0}{R}} \frac{r_0^{\frac{7-p}{2}}}{R} \cosh; \quad (5.13)$$

One can check that the $p = 3$ case agrees with the results in Sec. 3.1. However, for $p \notin 3$, the screening length does not behave as $r_0^{1=(p+1)}$ as one can see from Eq. (5.11). This is partly related to the fact that the Dp-brane sometimes ceases to be a $(p+1)$ -dimensional theory. For example, the D4-brane is a 6-dimensional theory in disguise. In fact, setting $p = 4$, one gets $L_s = (r_0 \cosh^2)^{-1=6}$. This is precisely the result one would expect for a 6-dimensional (conformal) theory.

As is well-known, such a transition does occur since the type IIA description becomes a bad description in the ultraviolet (as $r \rightarrow 1$), and the M-theory description takes over. The M5-brane, which is conformal, becomes the natural object to consider. So, this behavior is intimately related to the fact that the Dp-brane is nonconformal. The deviation from the conformal value is

$$L_s^{Dp} - \frac{1}{p+1} = \frac{(p-3)}{2(7-p)(p+1)} \rho_0; \quad (5.14)$$

so the exponent is always smaller than the conformal value (except $p = 3$).

6. Discussion

We found that the leading behavior of the screening length for conformal theories is given by $(\text{boosted energy density})^{-1/d}$. This behavior does not survive for nonconformal theories. Thus, in principle, we would not expect that $L_s / (\text{boosted energy density})^{-1/d}$ will apply for QCD. However, lattice results indicate that the speed of sound becomes close to $1/3$ for $T \gg 2T_c$ (see Ref. [36] for a summary of results by various groups). This implies that QCD may be approximately regarded as a conformal theory for such a range of temperatures. And this is precisely the range of temperatures of current and near-future experiments. Therefore, the conformal result may still be useful for modelling charm ionium suppression in heavy ion collisions. Even if the scaling exponent for QCD turns out to deviate from $1/d$, we expect the deviation to be proportional to the non-conformality parameter. It would be interesting to study the deviation from conformality for QCD at $T \gg 2T_c$ (theoretically and experimentally) and to find a gravity dual with an exponent similar to QCD.

Unlike QCD, none of the backgrounds studied here include dynamical quarks. Until recently only solutions with $N_f = N_c - 1$ were known. Lately, there has been an effort to find backgrounds that will include dynamical quarks beyond this approximation [37, 38, 39]. It would be interesting to explore the behavior of the screening length in these models.

We also found that the exponent becomes smaller than $1/d$ for nonconformal theories, but we do not have a precise understanding on the point. It would be interesting to check if this is also true for the other nonconformal theories and if QCD behaves similarly.

For $SAdS_5$ and R -charged black holes, the screening length in the ultrarelativistic limit is the same at a given energy density. As we saw in Sec. 3.2, only the leading behavior of the metric matters in the ultrarelativistic limit. Therefore the leading behavior depends only on the energy density, not on the charge.

The screening length at finite chemical potential is the same as the one at zero chemical potential, but one should keep in mind that this is valid only in the ultrarelativistic limit. They are certainly not the same for generic v . For arbitrary v , L_s is expected to be

$$L_s / \frac{f(v)}{1/d} (1 - v^2)^{1/d}; \quad (6.1)$$

where $f(v)$ is a slowly varying function of order one (by defining the function appropriately). A numerical computation is necessary to determine $f(v)$. We have carried out such an analysis as well and will present a detailed discussion of the numerical results elsewhere, but there are three things to be noted.

The function $f(v_R)$ is order one and $f(v_R) \rightarrow f(v_{R=0})$, where $f(v_R)$ and $f(v_{R=0})$ are the ones for finite chemical potential and for zero chemical potential, respectively.

The $f(v_R)$ -curve is approaching to $f(v_{R=0})$ in the ultrarelativistic limit as we saw in this paper.

The chemical potential dependence is very mild.

We hope that our analysis in the ultrarelativistic limit will be useful to understand the screening length behavior for different gauge theories.

7. Acknowledgments

It is a pleasure to thank Alberto Guijosa, Tetsuo Hatsuda, Tetsufumi Hirano, Kazunori Itakura, Kengo Mameda, Tetsuo Matsui, Osamu Morimatsu, and Berndt Müller for useful conversations. Elena Caceres thanks the Theory Group at the University of Texas at Austin for hospitality during the completion of this work. Her research is supported in part by the National Science Foundation under Grant Nos. PHY-0071512 and PHY-0455649, by Ramon Alvarez Bulla grant # 447/06 and CONACyT grant # 50760. The research of M.N. was supported in part by the Grant-in-Aid for Scientific Research (13135224) from the Ministry of Education, Culture, Sports, Science and Technology, Japan.

References

- [1] D. Teaney, "Effect of shear viscosity on spectra, elliptic flow, and Hanbury Brown-Twiss radii," *Phys. Rev. C* **68**, 034913 (2003).
- [2] T. Hirano and M. Gyulassy, "Perfect fluidity of the quark gluon plasma core as seen through its dissipative hadronic corona," *arXiv nucl-th/0506049*.
- [3] G. Policastro, D. T. Son and A. O. Starinets, "The shear viscosity of strongly coupled $N = 4$ supersymmetric Yang-Mills plasma," *Phys. Rev. Lett.* **87**, 081601 (2001) [*arXiv hep-th/0104066*].
- [4] P. Kovtun, D. T. Son and A. O. Starinets, "Holography and hydrodynamics: Diffusion on stretched horizons," *JHEP* **0310**, 064 (2003) [*arXiv hep-th/0309213*].
- [5] A. Buchel and J. T. Liu, "Universality of the shear viscosity in supergravity," *Phys. Rev. Lett.* **93**, 090602 (2004) [*arXiv hep-th/0311175*].
- [6] P. Kovtun, D. T. Son and A. O. Starinets, "Viscosity in strongly interacting quantum field theories from black hole physics," *Phys. Rev. Lett.* **94**, 111601 (2005) [*arXiv hep-th/0405231*].
- [7] A. Buchel, "On universality of stress-energy tensor correlation functions in supergravity," *Phys. Lett. B* **609**, 392 (2005) [*arXiv hep-th/0408095*].
- [8] J. Mas, "Shear viscosity from R -charged AdS black holes," *JHEP* **0603** (2006) 016 [*arXiv hep-th/0601144*].
- [9] D. T. Son and A. O. Starinets, "Hydrodynamics of R -charged black holes," *JHEP* **0603** (2006) 052 [*arXiv hep-th/0601157*].
- [10] O. Saremi, "The viscosity bound conjecture and hydrodynamics of M -brane theory at finite chemical potential," *arXiv hep-th/0601159*.
- [11] K. Mameda, M. Natsuume and T. Okamura, "Viscosity of gauge theory plasma with a chemical potential from AdS/CFT correspondence," *Phys. Rev. D* **73** (2006) 066013 [*arXiv hep-th/0602010*].
- [12] H. Liu, K. Rajagopal and U. A. Wiedemann, "Calculating the jet quenching parameter from AdS/CFT," *arXiv hep-ph/0605178*.
- [13] C. P. Herzog, A. Karch, P. Kovtun, C. Kozaç and L. G. Yaşar, "Energy loss of a heavy quark moving through $N = 4$ supersymmetric Yang-Mills plasma," *arXiv hep-th/0605158*.

- [33] A. Buchel, "Finite temperature resolution of the Klebanov-Strömberg singularity," Nucl. Phys. B 600 (2001) 219 [arXiv:hep-th/0011146].
- [34] L. A. Pando Zayas and C. A. Terrero-Escalante, "Black holes with varying flux: A numerical approach," arXiv:hep-th/0605170.
- [35] K. Mada, M. Natsuume and T. Okamura, "Quasinormal modes for nonextremal Dp-branes and thermalizations of super-Yang-Mills theories," Phys. Rev. D 72, 086012 (2005) [arXiv:hep-th/0509079].
- [36] F. Karsch, "Lattice QCD at high temperature and the QGP," arXiv:hep-lat/0601013.
- [37] R. Casero, C. Nunez and A. Paredes, "Towards the string dual of $N = 1$ SQCD-like theories," Phys. Rev. D 73, 086005 (2006) [arXiv:hep-th/0602027].
- [38] I. Kirsch and D. Vaman, "The D^3/D^7 background and flavor dependence of Regge trajectories," Phys. Rev. D 72, 026007 (2005)
- [39] B. A. Burrington, J. T. Liu, M. Mahato and L. A. Pando Zayas, "Towards supergravity duals of chiral symmetry breaking in Sasaki-Einstein cascading quiver theories," JHEP 0507 (2005) 019 [arXiv:hep-th/0504155].